

# Recognition of Wrist Position While Walking by Using Wearable Triaxial Accelerometers

Kaoru Furumi, Shintaro Mizoguchi, Nanako Niioka, Masashi Imai, and Atsushi Kurokawa\*

Hirosaki University  
3 Bunkyo, Hirosaki, Aomori 036-8561, Japan  
E-mail: \*kurokawa@eit.hirosaki-u.ac.jp

**Abstract:** Human activity recognition using wearable devices is becoming increasingly important. Techniques that estimate and recognize walking states while walkers carry an object in hand can be useful for safety and security. In this paper, we examine the recognition of walking states while walkers carry an object like a shoulder bag from data obtained by attaching a triaxial accelerometer to the wrists of walkers. The experimental results demonstrate that some states can be roughly identified from the accelerations and power spectrums.

*Keywords--* Human activity recognition, Wearable device, Accelerometer

## 1. Introduction

As the average life span increases, interest in health has likewise increased. The need to recognize human activity increases more and more as demand increases for a securer and safer life. Techniques for activity recognition using wearable devices are currently being researched [1-4]. For medicine, nursing, and health, many techniques related to the recognition of basic activity patterns such as walking, running, and going up and down stairs have been reported [5-10]. Moreover, recognitions of more complicated actions such as hand movements, daily life activity, sports, and fall detection have also been reported [4, 11-14]. With rapid advances in information and communications technology, wearable devices using not only accelerometers, but also gyroscopes, global positioning system (GPS), magnetometers, barometers, light sensors, temperature sensors, and image sensors have become available [1-4, 12, 15, 16]. To more accurately recognize human motions, research has been reported concerning installed sensors on many anatomical regions of the human body [1, 16, 17]. For example, by providing multiple sensors in many places, a method to recognize the movement of the arm has been presented [17]. However, on taking practical uses into account, users have a preference for fewer sensors because of their low cost, small size, and ease of use. Recognition of walking with objects such as shoulder bags and carry bags has barely been reported. Techniques that recognize the arm state while walking and estimate the object which a walker has are available in various fields such as crime prevention and behavior monitoring.

In this paper, we address activity recognition when walking with an object in hand. A triaxial accelerometer is attached to the wrists of walkers as a watch would be, and features are extracted from acceleration data. We demonstrate that a good recognition result is obtained by using accelerations and power spectrums in each direction. Although the sensor was attached to the left wrists of

walkers in this experiment, we assume that the sensors are attached to both wrists for practical use.

The rest of this paper is organized as follows. Section 2 describes the experimental method. Section 3 presents the feature extraction and experimental results. Finally, Section 4 concludes this paper.

## 2. Experimental Method

We describe measurement conditions and walking states as an experimental method.

### 2.1 Measurement Conditions

A wearable device is attached to the wrist of a walker as an arm watch would be. The device used in this paper is shown in Fig. 1(a). The device is composed of a triaxial accelerometer sensor module ADXL335 (Analog Devices, sampling frequency of 20 Hz, measurement range of  $\pm 3$  G) and wireless module XBee (Digi International, communication speed of 250 Kbps). The XYZ directions express the positive axes of the accelerometer.

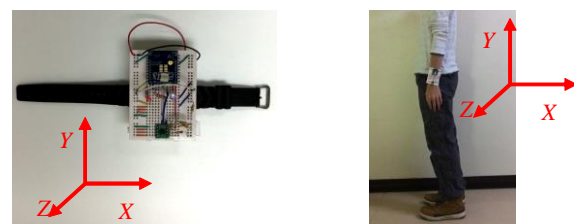
An example of the attached state is shown in Fig.1(b). In the standing state, the X, Y, and Z axes almost correspond to accelerations in the back and forth, up and down, and right and left directions, respectively. In this experiment, we collect acceleration data from eleven subjects, ten men and one woman.

### 2.2 Walking States

The walking states that are described in this paper are shown in Fig. 2. As walking states while walkers carry an object, we selected seven states.

The meanings of each state in Fig. 2 are as follows:

- (a) NO: Normal, walking naturally (empty-handed);
- (b) SB: Walking while holding the shoulder string of a shoulder bag by hand;
- (c) CB: Walking while pulling a carry bag;
- (d) UM: Walking with an umbrella up;



(a) Device

(b) Attached state

Figure 1. Wearable device used in this paper.

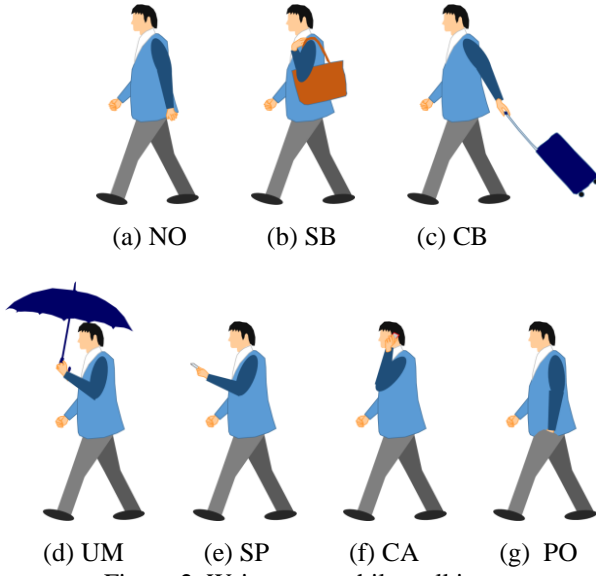


Figure 2. Wrist states while walking.

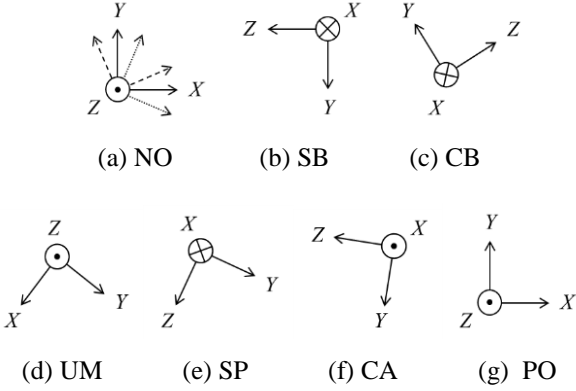


Figure 3. Directions of triaxial accelerometer sensor.

- (e) SP: Walking while watching the screen of a smartphone;
- (f) CA: Walking while making a call;
- (g) PO: Walking with a hand in a pocket.

Figure 3 shows the directions of a triaxial accelerometer on the wrist for each walking state. The directions except for NO (normal) and PO (pocket) are clearly different. Walking states except for NO are almost maintaining their wrist positions.

### 3. Features and Results

We describe features of each walking state and experimental results.

#### 3.1 Time Domain Features

An example of raw accelerometer data is shown in Fig. 4, which represents subject data for 5 sec. In the figure,  $X$ ,  $Y$ , and  $Z$  are the accelerations in the  $X$ ,  $Y$ , and  $Z$  directions, respectively.  $C$  is the composite and can be calculated from

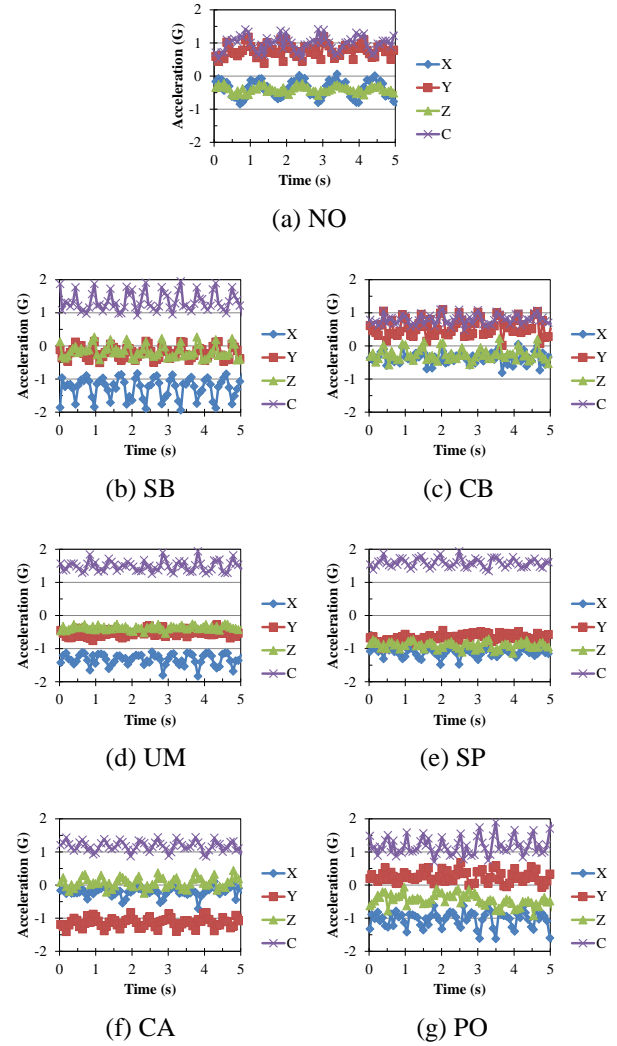


Figure 4. Example of raw accelerometer data for one subject.

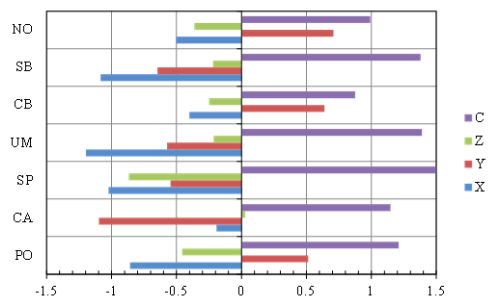


Figure 5. Acceleration average for eleven subjects.

$$\alpha_C = \sqrt{\alpha_X^2 + \alpha_Y^2 + \alpha_Z^2} . \quad (1)$$

Here,  $\alpha$  represents the acceleration. For example, the acceleration characteristics in Fig. 4(b) seem to be close to those in Fig. 4(a). However, the characteristics are clearly different from the characteristics of the other walking states.

The mean in each direction can be expressed as

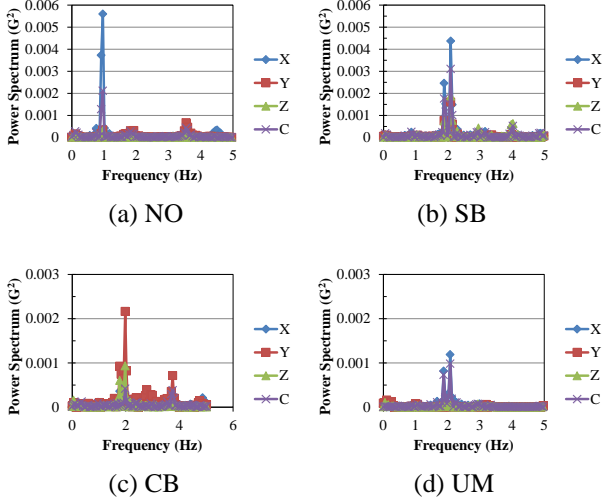


Figure 6. Example of power spectrum for one subject.

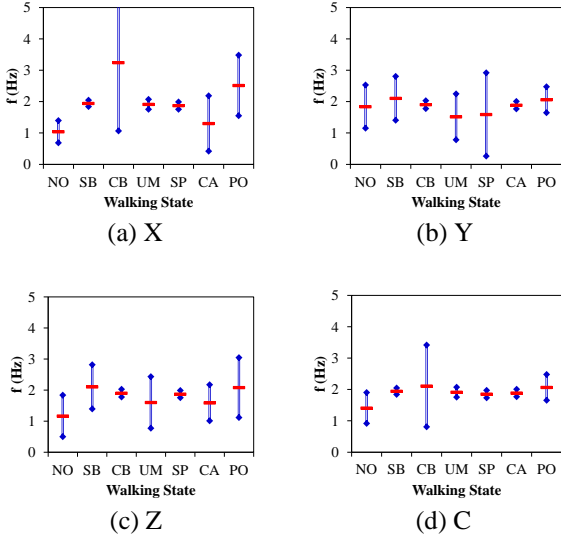


Figure 7.  $\mu_f$  and  $\pm\sigma_f$  of frequencies in which power spectrum reaches maximum for eleven subjects.

$$\mu_{\alpha_\beta} = \frac{1}{n} \sum_{i=1}^n \alpha_{\beta_i}, \quad (2)$$

where  $\alpha$  represents the acceleration, frequency, or power spectrum,  $\beta$  is the  $X$ ,  $Y$ ,  $Z$ , or  $C$ , and  $n$  is the sampling number. Figure 5 shows the average of the acceleration data for each state, obtained by eleven subjects. From the figure, we can see that the differences in the direction of  $Y$  and the magnitude of accelerations of  $X$  and  $Y$  appear as features.

### 3.2 Frequency Domain Features

For frequency domain features, we get characteristics of power spectrums obtained by fast Fourier transform (FFT) using a window size of 128 samples. Figure 6 shows an example of characteristics of power spectrum vs. frequency.

Figure 7 shows the mean  $\mu_f$  and standard deviation  $\pm\sigma_f$  of the frequencies in which power spectrum reaches the maximum. The standard deviation can be expressed as

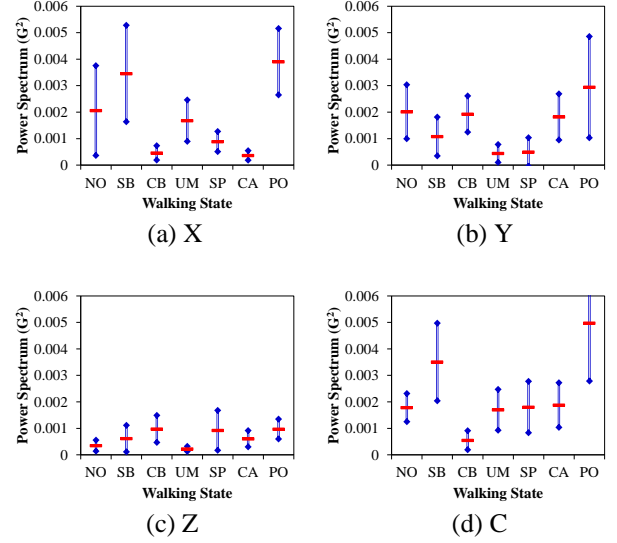


Figure 8.  $\mu_p$  and  $\pm\sigma_p$  of maximum power spectrums for eleven subjects.

Table 1. Extracted and selected features.

|       | NO              | SB      | CB              | UM      | SP    | CA    | PO     |
|-------|-----------------|---------|-----------------|---------|-------|-------|--------|
| $A_X$ | >-0.71          | <-0.74  | >-0.71          | <-0.74  | <-0.4 | >-0.5 | <-0.71 |
| $A_Y$ | >0.25           | <0      | >0.25           | <0      | <0    | <-0.5 | >0     |
| $A_Z$ | >-0.54          | >-0.6   | >-0.54          | >-0.6   | <-0.6 | >-0.5 | >-0.67 |
| $F_X$ |                 |         | >1.53           |         |       |       |        |
| $F_Y$ | >2.14,<br><1.89 |         |                 |         |       |       |        |
| $F_Z$ | >2.14,<br><1.63 |         |                 |         |       |       |        |
| $F_C$ |                 |         | >2.35,<br><0.31 |         |       |       |        |
| $P_X$ | >0.0011         | >0.0033 |                 | <0.0033 |       |       |        |
| $P_Y$ |                 | >0.0012 |                 | <0.0012 |       |       |        |
| $P_Z$ |                 | >0.0004 | >0.0008         | <0.0004 |       |       |        |
| $P_C$ | >0.0012         | >0.0033 | <0.0009         | <0.0033 |       |       |        |

Table 2. Identification results.

|                         | NO | SB | CB | UM | SP | CA  | PO |
|-------------------------|----|----|----|----|----|-----|----|
| Correct answer rate (%) | 91 | 73 | 91 | 82 | 82 | 100 | 91 |

$$\sigma_{\alpha_\beta} = \sqrt{\frac{1}{n-1} \sum_{i=1}^n (\alpha_{\beta_i} - \mu_{\alpha_\beta})^2}. \quad (3)$$

In Fig. 7, the red mark shows the mean and the top and bottom of the blue line are respectively  $+\sigma_f$  and  $-\sigma_f$ . SB, UM, and SB from Fig. 7(a) ( $X$  axis), CB and CA from Fig. 7(b) ( $Y$  axis), CB and SP from Fig. 7(c) ( $Z$  axis), and SB, UM, SP, and CA from Fig. 7(d) (composite) are in narrow frequency ranges. In addition, NO in the  $X$  axis is lower in frequency.

Figure 8 shows the mean  $\mu_p$  and standard deviation  $\pm\sigma_p$  of the maximum power spectrums. From Fig. 8(b) ( $Y$  axis), UM is lower in power spectrum. From Fig. 8(c) ( $Z$  axis), UM is lower in power spectrum, and CB is higher in power spectrum. From Fig. 8(d) (composite), CB is lower in power spectrum.

### 3. 3 Identification Results

From these feature extractions, we select features and determine boundaries of selected features. Table 1 lists the kind and the discrimination condition of the features.  $A_X$ ,  $A_Y$ , and  $A_Z$  stand for accelerations in the  $X$ ,  $Y$ , and  $Z$  directions.  $F_X$ ,  $F_Y$ ,  $F_Z$ , and  $F_C$  stand for frequencies in the  $X$ ,  $Y$ , and  $Z$  axes and composite.  $P_X$ ,  $P_Y$ ,  $P_Z$ , and  $P_C$  stand for power spectrums in the  $X$ ,  $Y$ , and  $Z$  axes and composite. The accelerations of the  $XYZ$  axes are used for all walking states.

Only from the acceleration average can we distinguish SP, CA, and PO. In other words, seven walking states are classified into five groups by the accelerations of the  $XYZ$  axes. The remaining states are distinguished by considering the frequency and power spectrum. As shown in Table 2, the identification results using the proposed method are good, correct answer rates.

## 4. Conclusion

We focused on walking state recognition when walking with an object in hand and examined feature extraction when by attaching a triaxial accelerometer to the wrists of walkers. By determining threshold conditions from the average of accelerations, the mean and standard deviation of frequencies of a maximum power spectrum, and the mean and standard deviation of maximum power spectrums, we showed that the seven walking states assumed in this paper can be estimated. Although recognition is based on the attributive conditions, and distinguishing similar states may be difficult, the proposed method is applicable to some extent for predicting a walking state with an object in hand.

## References

- [1] O.D. Lara and M.A. Labrador, "A survey on human activity recognition using wearable sensors," *IEEE Commun. Surveys Tuts.*, vol.15, no.3, pp.1192-1209, Jul. 2013.
- [2] J. Andreu-Perez, D.R. Leff, H.M.D. Ip, and G.-Z. Yang, "From wearable sensors to smart implants - toward pervasive and personalized healthcare," *IEEE Trans. Biomed. Eng.*, vol.62, no.12, pp.2750-2762, Apr. 2015.
- [3] T. Prajapati, N. Bhatt, and D. Mistry, "A survey paper on wearable sensors based fall detection," *International Journal of Computer Applications*, vol.115, no.13, pp.15-18, Apr. 2015.
- [4] X. Su, H. Tong, and P. Ji, "Activity recognition with smartphone sensors," *Tsinghua Science and Technology*, vol.19, no.3, pp.235-249, Jun. 2014.
- [5] D.M. Karantonis, M.R. Narayanan, M. Mathie, N.H. Lovell, and B.G. Celler, "Implementation of a real-time human movement classifier using a triaxial accelerometer for ambulatory monitoring," *IEEE Trans. Inf. Technol. Biomed.*, vol.10, no.1, pp.156-167, Jan. 2006.
- [6] J.R. Kwapisz, G.M. Weiss, and S.A. Moore, "Activity recognition using cell phone accelerometers," *ACM SigKDD Explorations Newsletter*, vol.12, no.2, pp.74-82, 2011.
- [7] M. Nguyen, L. Fan, and C. Shahabi, "Activity recognition using wrist-worn sensors for human performance evaluation," *Proc. of the IEEE ICDMW*, 164-169, 2015.
- [8] S.J. Preece, J.Y. Goulermas, L.P.J. Kenney, and D. Howard, "A comparison of feature extraction methods for the classification of dynamic activities from accelerometer data," *IEEE Trans. Biomed. Eng.*, vol.56, no.3, pp.871-879, Mar. 2009.
- [9] Y. Kurihara, K. Watanabe, and M. Yoneyama, "Estimation of walking exercise intensity using 3-D acceleration sensor," *IEEE Trans. Syst., Man, Cybern. C, Appl. Rev.*, vol.42, no.4, pp.495-500, Jul. 2012.
- [10] P. Gupta and T. Dallas, "Feature selection and activity recognition system using a single triaxial accelerometer," *IEEE Trans. Biomed. Eng.*, vol.61, no.6, pp.1780-1786, Jun. 2014.
- [11] R. Srivastava and P. Sinha, "Hand movements and gestures characterization using quaternion dynamic time warping technique," *IEEE Sensors J.*, vol.16, no.5, pp.1333-1341, Mar. 2016.
- [12] H. Kalantarian, N. Alshurafa, and M. Sarrafzadeh, "Detection of gestures associated with medication adherence using smartwatch-based inertial sensors," *IEEE Sensors J.*, vol.16, no.4, pp.1054-1061, Feb. 2016.
- [13] M. Ermes, J. Parkka, J. Mantyjarvi, and I. Korhonen, "Detection of daily activities and sports with wearable sensors in controlled and uncontrolled conditions," *IEEE Trans. Inf. Technol. Biomed.*, vol.12, no.1, pp.20-26, Jan. 2008.
- [14] X. Ma, H. Wang, B. Xue, M. Zhou, B. Ji, and Y. Li, "Depth-based human fall detection via shape features and improved extreme learning machine," *IEEE J. Biomed. Health Inform.*, vol.18, no.6, pp.1915-1922, Nov. 2014.
- [15] D. Roetenberg, H. J. Luinge, C. T. M. Baten, and P. H. Veltink, "Compensation of magnetic disturbances improves inertial and magnetic sensing of human body segment orientation," *IEEE Trans. Neural Syst. Rehabil. Eng.*, vol.13, no.3, pp.395-405, Sep. 2005.
- [16] S.J. M. Bamberg, A.Y. Benbasat, D.M. Scarborough, D.E. Krebs, and J.A. Paradiso, "Gait analysis using a shoe-integrated wireless sensor system," *IEEE Trans. Inf. Technol. Biomed.*, vol.12, no.4, pp.413-423, Jul. 2008.
- [17] G.X. Lee, K.S. Low, and T. Taher, "Unrestrained measurement of arm motion based on a wearable wireless sensor network," *IEEE Trans. Instrum. Meas.*, vol.59, no.5, pp.1309-1317, May 2010.